

View Article Online

EES Batteries

Accepted Manuscript

This article can be cited before page numbers have been issued, to do this please use: C. RENAIS, C. Villevielle, P. Peljo, F. El BACHRAOUI and H. Girault, *EES Batteries*, 2025, DOI: 10.1039/D5EB00202H.



This is an Accepted Manuscript, which has been through the Royal Society of Chemistry peer review process and has been accepted for publication.

Accepted Manuscripts are published online shortly after acceptance, before technical editing, formatting and proof reading. Using this free service, authors can make their results available to the community, in citable form, before we publish the edited article. We will replace this Accepted Manuscript with the edited and formatted Advance Article as soon as it is available.

You can find more information about Accepted Manuscripts in the <u>Information for Authors</u>.

Please note that technical editing may introduce minor changes to the text and/or graphics, which may alter content. The journal's standard <u>Terms & Conditions</u> and the <u>Ethical guidelines</u> still apply. In no event shall the Royal Society of Chemistry be held responsible for any errors or omissions in this Accepted Manuscript or any consequences arising from the use of any information it contains.



View Article Online DOI: 10.1039/D5EB00202H

As global efforts intensify to advance energy storage for decarbonized transport and grid resilience, lithium-ion batteries remain at the forefront due to their high energy density and scalability. Graphite, the dominant negative electrode material, has been central to their success, yet its fundamental electrochemical behavior is often oversimplified. This article revisits graphite's role from a mechanistic and thermodynamic standpoint, challenging its traditional classification as an anode. By dissecting the sequence of lithium insertion processes—from surface adsorption to underpotential deposition—the authors reveal that most stages lack true redox character. This nuanced understanding reshapes how graphite is conceptualized in battery science and underscores the need for precise definitions in developing next-generation storage materials.

Satteries Accepted Manuscrip

This article is licensed under a Creative Commons Attribution 3.0 Unported Licence

View Article Online DOI: 10.1039/D5EB00202H

ARTICLE

Redox aspects of lithium-ion batteries. Is graphite an anode?

Corentin Renaisa, Claire Villevieillea, Pekka Peljob, Fatima ElBachraouic, and Hubert Giraultc,d

Received 00th January 20xx. Accepted 00th January 20xx

DOI: 10.1039/x0xx00000x

Graphite is the most commonly used negative electrode in lithium-ion batteries. This perspective article reviews the charge transfer aspects of the graphite electrode, presenting the different mechanisms of graphite electrode involved during its charging from an electrochemical standpoint. Different reaction mechanisms can be distinguished: 1. Adsorption of solvated lithium ions on negatively charged graphite, 2. Intercalation of de-solvated lithium ions in graphite as a solid solution, 3. Biphasic (liquid-solid) formation of solid LiC36 and LiC12 phases, 4. Biphasic (solid-solid) formation of a LiC6 phase and 4. Under potential deposition of lithium atoms on the LiC₆ phase, which may be followed by classical electroplating of Li⁺ on Li. Only the last electrodeposition reactions are truly a redox process. The first three mechanisms represent the potentiometric titration of carbon sites for lithium ions intercalation.

1. Introduction

batteries are currently the most advanced electrochemical energy storage systems, essential for both stationary storage and e-mobility.

In a previous communication, we have addressed the redox reactions at the cathode1 and discussed the electrochemical aspects of the so-called "cathode material". Here, we shall discuss from an electrochemical viewpoint the charge transfer reactions taking place at the negative electrode.

Graphite negative electrodes remain the most widely commercialised material due to their excellent electrochemical properties. As an electroactive material, graphite offers a low working potential (close to that of lithium metal), is costeffective, environmentally friendly, and delivers a reasonable specific charge (372 mAh/g) over a large number of cycles.

This longevity is primarily attributed to a specific surface reaction known as the solid electrolyte interphase (SEI), which forms during the initial cycle and protects the graphite from further electrolyte decomposition. Although SEL

advantageous for graphite in today's commercial systems, it presents challenges for other high-energy-density technologies, such as the 5 V positive electrode. In these systems, transition metal leaching at high potential migrates to the SEI layer, initiating nucleation and rendering the SEI unstable, ultimately leading to poor electrochemical performance.

Similarly, alternative electroactive materials like silicon have demonstrated the ability to deliver exceptionally high specific capacity, up to ten times that of graphite. However, their alloying process, combined with a low potential and significant volume changes during cycling, results in unstable SEI formation, which has hindered their commercialisation so far. Despite years of intensive research, graphite continues to pose challenges for the development of next-generation Li-ion batteries. These challenges stem from its complex reaction mechanisms, multiple phase transitions during cycling, and unclear solid-state charge transport processes, that hinder highpower applications.

Nevertheless, the graphite negative electrode remains the most commercially viable option. To enhance its specific charge, graphite is currently combined with silicon nanomaterials to increase its specific energy. However, an excessive amount of silicon results in poor long-term electrochemical performance. In a previous communication, we explored the redox aspects of lithium-ion batteries, focusing on the metal oxide redox solids present at the positive electrode. Here, we will examine the electrochemical reactions occurring within the graphite negative electrode and ask whether it is, strictly speaking, an 'anode.'

a. Univ. Grenoble Alpes, Univ. Savoie Mont Blanc, CNRS, Grenoble INP, LEPMI,

b. Department of Chemistry and Materials Science, Aalto University, P.O. Box 16100 Aalto, Espoo, 00076 Finland.

c. Material Science, Energy and Nanoengineering (MSN) department, University Mohammed VI Polytechnic, 43 150 Ben Guerir, Morocco

d. Institute of Chemical Science and Engineering, Station 6, Ecole Polytechnique Federale de Lausanne, CH-1015 Lausanne, Switzerland

[†] Footnotes relating to the title and/or authors should appear here. Supplementary Information available: [details of any supplementary information available should be included here]. See DOI: 10.1039/x0xx00000x

Open Access Article. Published on 30 Onkololeessa 2025. Downloaded on 09/11/2025 7:31:13 AM.

This article is licensed under a Creative Commons Attribution 3.0 Unported Licence

ARTICLE

2. Graphite charging stages

The graphite electrode is indeed a major component of most lithium ion-batteries. It has been thoroughly discussed and reviewed². Nonetheless, it remains a topic of active research both theoretically and experimentally, particularly using *in operando* techniques. Graphite lithiation is usually described by the Daumas-Herold³ or Rüdorff-Hofman⁴ nomenclatures, which categorise the different lithiation stages based on the number of graphite layers separating the lithium cation layers.

In the so-called dilute stages, lithium is sparsely distributed, and these stages are described as 'liquid-like' (often denoted by 'L' to indicate the liquid-like phase). In contrast, during the dense stages, lithium layers become ordered, adopting a 'solid-like' structure.

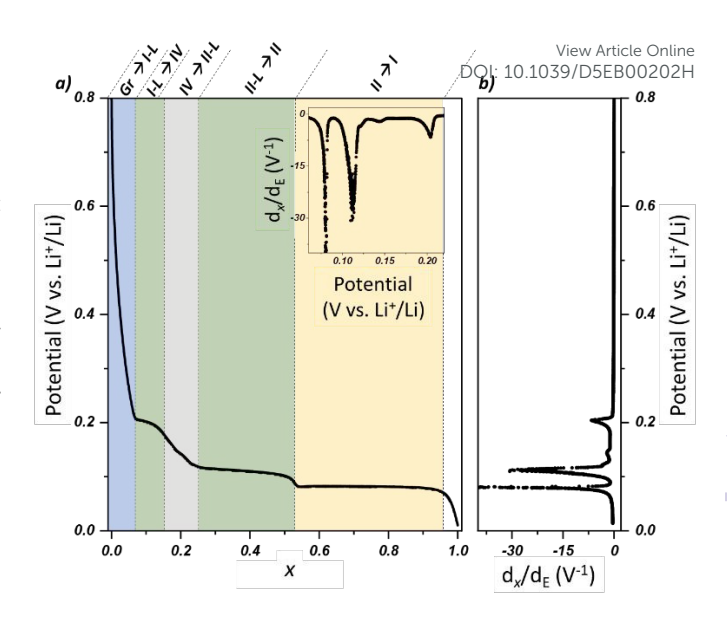
Starting from the fully lithiated LiC_6 phase, the different stages are as follows:

- Stage 1, the more densely packed and fully lithiated graphite, is a LiC₆ phase, which has a theoretical specific capacity of 372 mAh/g,
- Stage 2 is also a pure solid phase in which fully lithiated layers are separated by two graphite layers. It can be described as a LiC₁₂ phase.
- Stage 2-L is a solid solution in which no in-plane order is observed.
- Stages 3, 4 are solid phases and are characterised by lithiated layers separated by 3 and 4 graphite layers, respectively. Stage 4 can be described as LiC₃₆ phase.
- Stage 1-L is a solid solution with every interlayer filled with lithium ions but in a diluted manner, as a diluted stage 1. No in-plane order is observed.
- Stage P is the pristine graphite form.

The different lithiation stages are illustrated in Figure 1a, which presents the galvanostatic curve of a graphite electrode cycled against a lithium metal electrode, which serves as both the reference and the counter electrode. As such, this graph represents a potentiometric titration curve of the different intercalation sites.

The graphite lithiation profile exhibits distinct features in terms of potential evolution, which have been extensively described since the 1990s. Three primary potential plateaus are observed, corresponding to x = [0.08-0.16], [0.25-0.52] and [0.52-0.95] (± 0.01), note that stage II is observed for $x \approx 0.52$ and not for 0.5. This difference comes from the adsorbed charges and the charges involved in the SEI that are considered in the overall electronic charge (x), slightly increasing the specific capacity of graphite. The associated phase transitions are indicated at the top of Figure 1a.

Differential capacity analysis (DCA), as shown in the inset of Figure 1a and in Figure 1b, provides valuable information on the lithium intercalation mechanism.



Journal Name

Figure 1: a) Voltage profile for constant-current cycling of a Li | graphite half-cell (vs Li metal) between 1.2 V - 0.01 V and representation of the different stages of graphite lithiation, where x represents the proportion of the overall electronic charge that can be stored. [Adapted from⁵]; b) the corresponding differential curves showing the different graphite stages.

For instance, it is widely recognised that a solid-solid biphasic state occurs within the range x = 0.52 - 0.95 (yellow zone), where LiC₆ phases (stage I) progressively form from LiC₁₂ phases (stage II). This solid-solid biphasic mechanism, observed in various insertion materials such as LiFePO₄, is characterised by the coexistence of two pure solid phases with constant chemical potentials, meaning that the composition of each phase remains unchanged, only their volume is changing. In such a first-order transition, the cell voltage is expected to be constant because of the coexistence of two pure phases. Consequently, a divergence of d_x/d_E should be observed in DCA^{6,7}. Experimentally, within the yellow zone (Figure 1a), the potential evolution remains remarkably flat, and the corresponding DVA peak is narrow. However, kinetic effects induce a slight potential decrease, preventing a true divergence. In contrast, within the green zones attributed to "solid solution-solid" reactions (as discussed below), the potential evolution is more pronounced, and larger peaks appear in the DVA representation. The distinction between the green and yellow zones underscores the differences in lithium intercalation reaction mechanisms, i.e. solid solution-solid and solid-solid, which are responsible for differences in potential evolution — a topic further explored in the following sections.

3. Graphite charging - electrochemical modelling

To electrochemically model the charging process of a graphite electrode, we must consider several key steps. The first involves the adsorption of solvated lithium cations onto the graphite surface. Next, these cations undergo desolvation and intercalation, becoming sparsely distributed across certain layers—lacking true structural order apart from a superstructure before condensing into specific phases.

Accepted Manuscrip

Journal Name ARTICLE

To distinguish these different steps, we will consider an electrochemical cell model comprising a pristine graphite electrode (G) and a lithium metal electrode, separated by an electrolyte solution (S) containing a lithium salt (Li^+A^-) as given by **Cell I**.

Cell I:

 M^{I} | Lithium metal (Li) | Lithium electrolyte (S) | Graphite (G) | M^{II}

The cell voltage, which can be measured experimentally using a simple voltmeter, is defined as the Galvani potential difference between the two current collectors (M^I and M^{II}) made of the same metal and connected to the graphite and lithium electrodes, respectively. The cell voltage is expressed in Eq. 1:

$$\begin{split} [E]_{\text{vs Li}^{+}/\text{Li}} &= \phi^{\text{M}^{\text{II}}} - \phi^{\text{M}^{\text{I}}} \\ &= (\phi^{\text{M}^{\text{II}}} - \phi^{\text{G}}) + (\phi^{\text{G}} - \phi^{\text{S}}) + (\phi^{\text{S}} - \phi^{\text{Li}}) + (\phi^{\text{Li}} - \phi^{\text{M}^{\text{I}}})_{(1)} \end{split}$$

where ϕ represents the Galvani potential, also called the inner potential of the different phases in contact. To proceed, we must define the electrochemical potential of the electron as the energy required to bring an electron from vacuum into a given phase, which is expressed by Eq. 2^8 .

$$\tilde{\mu}_{e^{-}} = \mu_{e^{-}} - F\chi - F\psi = \mu_{e^{-}} - F\phi = -\Phi - F\psi$$
 (2)

where μ_- represents the chemical potential of the electron, χ the surface potential of the phase and ψ the outer potential of the phase associated to the presence of an excess charge on its surface. Φ represents the work function, the work to extract an electron from an uncharged phase. Φ defines the Fermi level of the electron in the phase with respect to vacuum. At the M $^{\parallel}$ | graphite junction, electrons can move freely, leading to equalization of the electrochemical potential of the electron in both M $^{\parallel}$ and graphite, as expressed in Eq. 3:

$$\phi^{M^{II}} - \phi^{G} = \left(\mu_{e^{-}}^{M^{II}} - \mu_{e^{-}}^{G}\right) / F \tag{3}$$

At the lithium counter/reference electrode, the Galvani potential difference between the lithium metal and the electrolyte solution (S) is given by considering the electrochemical redox equilibrium (Reaction I):

$$Li^{+S} + e^{-Li} \rightleftarrows Li$$
 (I)

At equilibrium, the electrochemical potentials of the reactants and the products are equal (Eq. 4):

$$\mu_{\text{Li}} = \widetilde{\mu}_{\text{Li}}^{\text{S}} + \widetilde{\mu}_{e^{-}}^{\text{Li}} \tag{4}$$

where $\mu_{\rm Li}$ represents the work that is done to add an atom of lithium to a pure lithium metal phase. By developing the electrochemical potential of an ionic species as follows (Eq. 5):

$$\widetilde{\mu}_{i} = \mu_{i} + z_{i}F\phi = \mu_{i}^{o} + RT\ln a_{i} + z_{i}F\phi$$
 (5)

the Galvani potential difference between the lithium metal and the electrolyte solution is given by (Eq. 6):

$$\phi^{S} - \phi^{Li} = \left(\mu_{Li} - \mu_{Li^{+}}^{o,S} - \mu_{e^{-}}^{Li}\right) / F - \frac{RT}{F} \ln a_{Li^{+}}^{S}$$
 (6)

 $\mu_{\mathrm{Li}^+}^{o,S}$ represents the work to bring a lithium cation from vacuum to the electrolyte solution under standard conditions (E.g. 4M), which is also the standard solvation energy, as illustrated below in Figure 2.

As shown by (Eq.2), $-\mu_{e^-}^{\rm Li}$ represents the work to extract an electron from the Fermi level of a neutral lithium metal, *i.e.* the work function of lithium (about 3.1 eV⁹) and where a is the activity of the lithium ion in the electrolyte solution; the activity of lithium in the metallic phase is unity as it is a pure metal. $\mu_{\rm Li}$ can be approximated as being minus the energy of sublimation of lithium, *i.e.* 159 kJ·mol⁻¹ (Wikipedia). To give an order of magnitude, the Gibbs solvation of Li⁺ in propylene carbonate solution was calculated to be around –540 kJ·mol⁻¹. 10

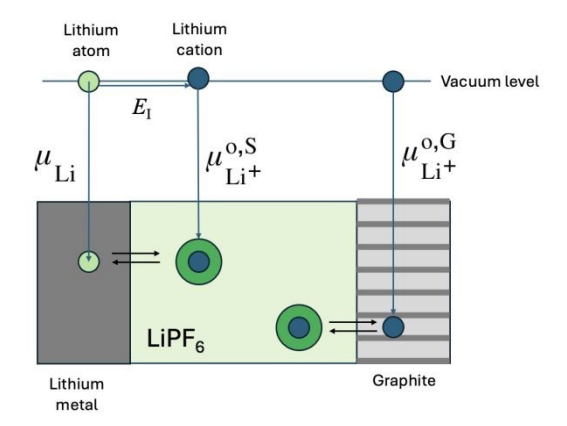


Figure 2: Thermodynamic cycle for lithium cation insertion in graphite, where $E_{\rm I}$ is the ionisation energy of a lithium atom. The green central zone represents the electrolyte solution

At the M^1 | lithium metal junction, electrons move freely, leading to the equalisation of the electrochemical potential of the electron in both the lithium metal and M^1 , as expressed in Eq. 7

$$\phi^{Li} - \phi^{M^{I}} = \left(\mu_{e^{-}}^{Li} - \mu_{e^{-}}^{M^{I}}\right) / F \tag{7}$$

Consequently, Eq. (1) simplifies to

$$[E]_{\text{vs Li}^{+}/\text{Li}} = \phi^{\text{M}^{\text{II}}} - \phi^{\text{M}^{\text{I}}}$$

$$= (\phi^{\text{G}} - \phi^{\text{S}}) + (\mu_{\text{Li}}^{-} - \mu_{\text{Li}^{+}}^{\text{o,S}} - \mu_{e^{-}}^{\text{G}}) / F - \frac{RT}{E} \ln a_{\text{Li}^{+}}^{\text{S}}$$
(8)

With this foundation established, we can now examine the graphite | electrolyte solution interface to express the first term of Eq.8.

3.1. Lithium adsorption on graphite

In the initial step of charging a pristine graphite particle, the electrode reaction can be defined as a simple electroadsorption process of a solvated lithium ion on an inert electrode, as illustrated in Figure 3a and expressed by Reaction II.

$$Li^{+,S} \iff Li^{+}_{ads}$$
 (II)

If in a first approximation we ignore the presence of surface groups such as oxides and the presence of the SEI, this is a

Open Access Article. Published on 30 Onkololeessa 2025. Downloaded on 09/11/2025 7:31:13 AM.

This article is licensed under a Creative Commons Attribution 3.0 Unported Licence

ARTICIF

Journal Name

purely capacitive process in which the outer potential of the graphite varies and the Fermi level of the electrons in graphite rises as the electrode becomes more electronegative. A Frumkin-type approach can be applied to calculate the potential difference in the electrolyte solution between the graphite surface and the bulk electrolyte.

Starting with the equalisation of the electrochemical potential of lithium ions between the bulk electrolyte solution and the graphite surface, we obtain Eq. 9:

$$\mu_{\text{Li}^{+}}^{\text{o,S}} + RT \ln a_{\text{Li}^{+}}^{\text{S}} + F\phi^{\text{S}} = \mu_{\text{Li}^{+}}^{\text{o,S}} + RT \ln a_{\text{Li}^{+}}^{\text{ads}} + F\phi^{\text{ads}}$$
(9)

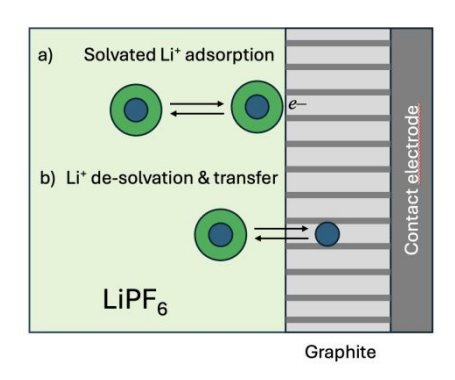


Figure 3: a) Schematic representation of the adsorption of a solvated lithium cation on the negatively charged surface of graphite. b) Schematic transfer of a lithium cation from the electrolyte solution, where it exists in a solvated state, to graphite, where it becomes a bare cation. By definition, the partially lithiated graphite phase remains electrically neutral overall as a result of the electrical charging of the graphite.

Therefore, the Galvani potential difference between the solution and the adsorption plane is described by Eq. 10.

$$\phi^{\text{ads}} - \phi^{\text{S}} = \frac{RT}{F} \ln \left(\frac{a_{\text{Li}^+}^{\text{S}}}{a_{\text{Li}^+}^{\text{ads}}} \right) \tag{10}$$

where ϕ and a represents the potential in the solution on the surface of the graphite electrode, where solvated lithium ions adsorb. The inner potential of the graphite particle phase varies with changes in the outer potential upon charging.

The polarised interface can be treated as a capacitor. For an ideally spherical graphite particle with radius R, the potential difference between the graphite and the adsorbed lithium layer is expressed by Eq. 11:

$$\phi^{G} - \phi^{ads} = Q/C \tag{11}$$

where the capacitance C can be written in a first approximation as in Eq. 12:

$$C = 4\pi\varepsilon R^2/\delta \tag{12}$$

where δ is the distance between the adsorbed solvated lithium ions and the graphite edge and ε the permittivity of this layer. The Frumkin adsorption isotherm expresses the surface coverage $\,\theta\,$ of the adsorbate to the bulk concentration c and can be expressed as in Eq. 13:

$$\theta = \frac{Kc}{1 + Kc} \exp^{-a\theta} \tag{13}$$

where K is the adsorption equilibrium constant and a is the parameter representing the interactions between the factor of the parameter representing the interactions between the factor of the parameter representing the interactions between the factor of the parameter representing the interactions between the factor of the parameter representing the interactions between the factor of the parameter representing the parameter representation representing the parameter representation re ions. The limiting form at low coverage reads simply (Eq. 14):

$$\theta = Kc \tag{14}$$

So, the charge of the particle is given by Eq. 15:

$$Q = \theta_{\text{Li}^+} Q_{\text{max}} = 4\pi R^2 \theta_{\text{Li}^+} \sigma_{\text{max}} \tag{15}$$

By substitution, we have Eq. 16:

$$\phi^{G} - \phi^{ads} = \theta_{Li} + \sigma_{max} / \varepsilon_{0}$$
(16)

All in all, the cell voltage of Cell I is given by Eq. (8) and can ther be translated into Eq. 17:

$$[E]_{\text{Li}^{+}/\text{Li}} = \phi^{\text{M}^{\text{II}}} - \phi^{\text{M}^{\text{I}}}$$

$$= \theta_{\text{Li}^{+}\sigma_{\text{max}}} / \varepsilon_{0} + \left(\mu_{\text{Li}}^{-} - \mu_{\text{Li}^{+}}^{\text{o,S}} - \mu_{e^{-}}^{\text{G}}\right) / F - \frac{RT}{F} \ln a_{\text{Li}^{+}}^{\text{ads}}$$
(17)

The dominant term in Eq. 17 is the last one, which shows that the potential decreases sharply as adsorption progresses.as observed at the start of the blue area in Figure 1a. As expected from adsorption processes on highly ordered materials, the amount of charge stored is relatively small, unless the materials are mesoporous. This simplified approach does not account for the formation of the SEI or surface chemistry effects, such as adventitious carbon.

The final value of x at the end of the surface adsorption step, as shown in Figure 1a, depends on several factors: i) The structural order of the material—if the graphite possesses disordered domains (such as in hard carbons), the adsorption process can be more extensive. ii) The surface roughness—a higher exposed surface area leads to increased adsorption. iii) The surface chemistry of graphite.

Typically, in conventional graphite electrodes, the adsorption process occurs for small values of x.

3.2. Lithium insertion in graphite - Ion transfer reactions

As discussed in the following, during the charging process, solid solutions of lithium ions in graphite are observed. Thermodynamically, a solid solution is characterised by a temperature dependence of the structure¹¹, here solid solution means that some lithium ions are free to move in the graphite

When the graphite presents a solid solution mechanism, lithium ions of the electrolyte solution undergo desolvation, and the bare lithium cation randomly intercalates between graphite sheets, as illustrated in Figure 3b and expressed in Reaction III.

$$Li^{+,S} \iff Li^{+,G}$$

Ion transfer reactions have been extensively studied at ITIES (Interface between Two Immiscible Electrolyte Solutions) for more than a century. These reactions are, in essence, electrochemical reactions, as they are controlled by an applied potential difference between the two phases.

Accepted Manus

Journal Name ARTICLE

Here, at the electrolyte solution | graphite interface, the equality of the electrochemical potentials reads as in Eq. 18:

$$\mu_{\text{Li}^{+}}^{\text{o,S}} + RT \ln a_{\text{Li}^{+}}^{\text{S}} + F\phi^{\text{S}} = \mu_{\text{Li}^{+}}^{\text{o,G}} + RT \ln a_{\text{Li}^{+}}^{\text{G}} + F\phi^{\text{G}}$$
(18)

The negatively charged graphite acts as a "solvent" for lithium cations. From Eq. (18), we can derive the Nernst equation for the lithium ion transfer⁷ reaction as given by Eq. 19.

$$\phi^{G} - \phi^{S} = \left(\mu_{\text{Li}^{+}}^{\text{o,S}} - \mu_{\text{Li}^{+}}^{\text{o,G}}\right) / F + \frac{RT}{F} \ln \left(\frac{a_{\text{Li}^{+}}^{S}}{a_{\text{Li}^{+}}^{G}}\right)$$
(19)

 $\mu_{r,+}^{o,S}$ and $\mu_{r,+}^{o,G}$ are illustrated in Figure 2 and represent the standard solvation energy of the lithium cation in its respective standard states. For the electrolyte solution, the standard state is typically defined by a concentration of 1 M, while for the solid solution graphite phase, it corresponds to a molar fraction of unity—i.e. a hypothetical fully charged 'solid solution' graphite. During the charge of the solid solution, the graphite electrode functions neither as a cathode nor as an anode, as no redox reactions occur. Instead, it operates as a porous electrode, charging via ion transfer/insertion under the applied potential and subsequently releasing charge through ion extrusion.

The key distinction from the simple solvated lithium cation adsorption described earlier in Eq. (17) lies in the desolvation/resolvation reaction occurring during insertion /extraction. Based on Eq. (8) and Eq. (19), the voltage of **Cell I** is then given by Eq. (20).

$$[E]_{\text{vs Li}^{+}/\text{Li}} = \left(\mu_{\text{Li}}^{-} - \mu_{\text{Li}^{+}}^{\text{o,G}} - \mu_{e^{-}}^{\text{G}}\right) / F - \frac{RT}{F} \ln a_{\text{Li}^{+}}^{\text{G}}$$
(20)

This potential difference is independent of the lithium concentration in the electrolyte. Eq. (20) is the "Master equation" expressing the potential dependence upon charging when some solid solution phases are present. It shows why the potential decreases upon lithium-ion insertion

 $\mu_{\rm Li^+}^{\rm o,G}$ can then be estimated from Eq. (20) using the thermodynamic cycle of Figure 2 with the following values:

- 160 kJ·mol⁻¹ (sublimation energy of lithium),
- 450 kJ·mol⁻¹ (estimated work function of graphite),
- 200 kJ·mol⁻¹ (experimental cell voltage at 0.2 V for the blue and grey zone taken as a first average approximation)

This yields an approximate value of –810 kJ·mol⁻¹, suggesting that graphite serves as a more effective 'solvent' for bare lithium cations compared to propylene carbonate (–540 kJ·mol⁻¹).

The dissolution of bare lithium cations in graphite, being an ion transfer reaction, allows graphite to be considered an "ionode," using the terminology proposed for ion transfer reactions at liquid | gel interfaces¹² Here, the ion transfer reaction occurs between an organic liquid electrolyte solution and a graphite phase exhibiting a "liquid-like" behaviour.

3.3. Lithium insertion in graphite- Biphasic system: "solid nline solution - solid" regions DOI: 10.1039/D5EB00202H

In the blue zone, the adsorbed lithium ions start to de-solvate and intercalate in the graphite. Experimental studies have shown that lithium can begin to intercalate into the graphite structure at potentials below 0.5 V vs Li $^+$ /Li¹³. When entering the first green zone at x = 0.08, the process is still being discussed in the literature about the nature of the Li_xC₆ compound. Based on Dahn's work in 1991¹¹, this intermediate is a diluted stage I, displaying no in-plane order with intercalants in every graphite interlayer. Following this hypothesis, some authors consider this phase as a solid solution^{14,15}. On the other hand, some consider this intermediate to be an 8th stage with lithium intercalant in every 8 graphite layer, supporting a "pure" solid phase¹⁶⁻¹⁸. Based on the electrochemical profile from x = 0.08 to 0.16, the hypothesis of a solid solution (stage 1-L) is preferred here as explained below.

Upon further insertion of lithium ions in the remaining free graphite, the lithium ions are mobile in a solid solution phase and a stage IV starts to form, or so to speak to precipitate to form LiC_{36}^{18} .

Similarly, at the end of grey zone, where the potential also varies rather strongly, the lithium ions are mobile in a solid solution stage II-L and a stage II starts to form.

In the two green zones (Figure 1a), the randomly distributed lithium ions in the solid solution "precipitate" to form a solid LiC_{36}^{18} and LiC_{12} phase, respectively. From a thermodynamic perspective, the reaction can be stoichiometrically expressed as Reactions IV and V:

$$\text{Li}^{+,S} + e^{-G} + 36 \text{ C}^{G} \iff \left[\text{Li}^{+}\text{C}_{36}^{-}\right]^{\text{LiC36}}$$
 (IV)

$$\text{Li}^{+,\text{S}} + e^{-\text{G}} + 12 \text{ C}^{\text{G}} \Longleftrightarrow \left[\text{Li}^{+\delta}\text{C}_{12}^{-\delta}\right]^{\text{LiC}12}$$
 (V)

where the reactants are a solvated lithium ion in the electrolyte solution, an electron from the graphite and 36 or 12 carbon atoms from the graphite structure, respectively.

In the case of LiC_{36} , the concentration of lithium in graphite is small enough to consider that the cation conserves its positive charge.

In the case of LiC₁₂, there are two limiting situations to consider: either as an ionic solid Li⁺C₁₂⁻ (δ = 1) or simply as a neutral solid (δ = 0). It is important to note that the Li-C interaction is probably partially ionic with (0 < δ < 1), but this falls beyond the scope of the present discussion. Regardless of the specific nature of the interaction, the phase remains globally neutral.

Reactions IV and V may appear to be a reduction reaction of the lithium cation, but in fact, they correspond to the formation of a neutral phase. For LiC₁₂, it can be interpreted as a partial reduction of Li⁺, where 0 < δ < 1. In this framework, graphite could be partially considered as an anode, although this interpretation extends beyond the strict IUPAC definition 19 .

From the perspective of electrochemical potentials, we can ascribe LiC_{36} and LiC_{12} as a homogeneous phase and write Eqs. 21 & 22.

ARTICIF

Journal Name

$$\left(\mu_{\text{Li}^+}^{\text{o,S}} + RT \ln a_{\text{Li}^+}^{\text{S}} + F\phi^{\text{S}}\right) + \left(\mu_{e^-}^{\text{G}} - F\phi^{\text{G}}\right) + 36 \,\mu_{\text{C}}^{\text{G}} = \mu_{\text{LiC36}} \tag{21}$$

$$\left(\mu_{\text{Li}^{+}}^{\text{o,S}} + RT \ln a_{\text{Li}^{+}}^{\text{S}} + F\phi^{\text{S}}\right) + \left(\mu_{e^{-}}^{\text{G}} - F\phi^{\text{G}}\right) + 12 \,\mu_{\text{C}}^{\text{G}} = \mu_{\text{LiC12}} \tag{22}$$

From which, using Eq. 8, we obtain the following equation (Eqs.23 & 24) for the end of the green zones (x = 0.16 & x=0.52 in Figure 1a).

$$[E]_{\text{vs Li}^+/\text{Li}} = \left(\mu_{\text{Li}}^- - \mu_{\text{LiC36}}^+ + 36 \,\mu_{\text{C}}^{\text{G}}\right) / F$$
 (23)

$$[E]_{\text{vs Li}^+/\text{Li}} = \left(\mu_{\text{Li}} - \mu_{\text{LiC12}} + 12\,\mu_{\text{C}}^{\text{G}}\right)/F$$
 (24)

Eq. (23 & 24) represents the equilibrium potential of homogeneous solid LiC36 & LiC12 electrodes immersed in a lithium electrolyte solution, measured against a lithium metal counter electrode, as shown in Cell II.

Cell II:

Open Access Article. Published on 30 Onkololeessa 2025. Downloaded on 09/11/2025 7:31:13 AM.

This article is licensed under a Creative Commons Attribution 3.0 Unported Licence

M^I | Lithium metal | Lithium electrolyte solution | LiC_{36/12} | M^{II}

To calculate the potential in the green zones (0.08 < x < 0.16 and 25 < x < 0.52, Figure 1a), Eq.(20) applies as we are partially in the presence of a solid solution phase, and we can draw an analogy with the potentiometric titration of silver cations in aqueous solutions, by adding KBr. In this widely used potentiometric titration, the potential of a silver electrode immersed in the electrolyte solution is governed by the Nernst equation of the Ag+/Ag couple. Upon addition of the titrant solution, AgBr begins to precipitate, leading to a decrease of the concentration of Ag+ concentration to its minimum value, determined by the solubility product, $K_{\rm S}$, of AgBr, such that $[Ag^{+}]_{min}=(K_{S})^{1/2}$, thus marking the endpoint of the reaction.

In the present case, we 'titrate' C₆ sites by introducing Li⁺ and electrons, and we can consider the 'precipitation' of LiC₃₆ or LiC₁₂ solids. The potential of **Cell I** remains governed by Eq. (20) since part of the phase persists as a solid solution, and the potential varies as the concentration of free lithium ions in the solid solution increases as the volume of the solid solution decreases due to the formation of the solid phases. The electric charge x in Figure 1a associated to inserted lithium ions in the graphite is no longer solely determined by the molar fraction of freely moving Li⁺ within the film—it also includes the fraction of 'precipitated' Li⁺, forming the LiC₃₆ & LiC₁₂ phases.

The variation in potential within the green zones, based on this redox titration approach, is further developed the Supplementary Information (SI) (see Eq. S6).

At x = 0.52, where the potential is defined by Eq. (24), the material consists of a pure solid phase of LiC₁₂, as schematically illustrated in Figure 4.

3.4. Lithium insertion in graphite- "Biphasic system: solid solid" region

Upon further charging, we have the following Reaction VI:

$$\text{Li}^{+,S} + e^{-G} + \text{LiC}_{12} \rightleftarrows 2 \text{LiC}_{6}$$
 (VI)

Again, by developing the electrochemical potentials of the different species, we obtain the Galvaniopatential difference between the electrolyte solution and the graphite (Eq. 23)

$$\begin{split} \phi^{\rm G} - \phi^{\rm S} &= \left(\mu_{\rm Li^+}^{\rm o,S} + \mu_{e^-}^{\rm G} + \mu_{\rm LiC12} - 2\,\mu_{\rm LiC6}\right) / F \\ &+ \frac{RT}{F} {\rm ln} a_{\rm Li^+}^{\rm S} \end{split} \tag{25}$$

By substituting in Eq. 8, we finally show that Cell I voltage is constant for x > 0.52 as we have two pure solid phases in contact, namely LiC₁₂ and LiC₆.

$$[E]_{\text{vs Li}^+/\text{Li}} = \phi^{\text{M}^{\text{II}}} - \phi^{\text{M}^{\text{I}}} = (\mu_{\text{Li}} + \mu_{\text{LiC12}} - 2 \mu_{\text{LiC6}})/F$$
 (26)

Eq. (26) is the equilibrium potential of a LiC₁₂/LiC₆ electrode immersed in a lithium electrolyte solution and measured versus a lithium metal counter electrode.

The formation of two pure solid phases LiC₁₂ and LiC₆ explained the flat voltage profile in Figure 1 for x > 0.52. The phases LiC₁₂ and LiC₆ have a strong metallic character, as illustrated by the golden and reflective colour of LiC₆ as reported, for example, by Gao et al.20.

It is interesting to note that from an electrochemical viewpoint, the potential response does not depend on the electronic structure of the pure phases.

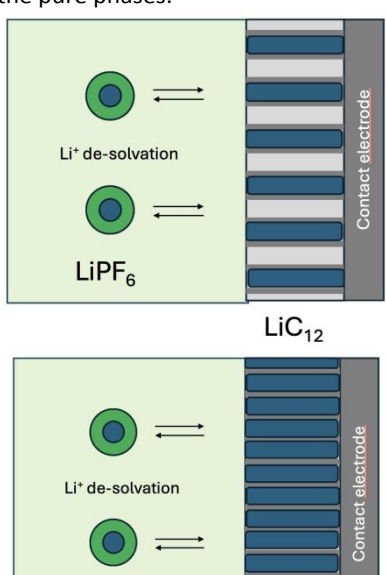


Figure 4: Schematic reaction between solvated lithium cation and the solid phase LiC₁₂ (top) and LiC₆ (bottom). The blue represents the graphite sheets filled to form a solid phase.

It is independent of the fact that the lithium cations are partially reduced, i.e., that electrons "visit" the 2s orbital of the bare lithium ions and hence contribute to the definition of the Fermi level.

3.5. Lithium metal deposition on LiC₆.

LiPF

Finally, once the graphite electrode is nearly fully lithiated (x=0.95), we can observe lithium metal under potential

LiC₆

Batteries Accepted Manuscril

Journal Name ARTICLE

deposition on the surface of the LiC_6 electrode at a potential of +80 mV. Under potential metal deposition (UPMD) has been studied for decades. It corresponds to the deposition of a monolayer of metal atoms "A" onto another metal substrate "B", at potentials more positive than the reversible Nernst potential of the deposition of metal "A" on "A", for example, as given by Eq. (I). In 1974, Kolb *et al.*²¹ had shown that the underpotential difference was proportional to the difference in the work functions of metals "A" and "B".

Compared to Cell I for the deposition of lithium on lithium, we have the deposition of lithium on LiC₆ as given by Reaction VI.

$$\text{Li}^{+\text{S}} + e^{-\text{LiC}_6} \rightleftarrows \text{Li}_{\text{UPD}}$$
 (VI)

For which we have

$$\mu_{\text{Li}_{\text{UPD}}} = \tilde{\mu}_{\text{Li}^+}^{\text{S}} + \tilde{\mu}_{e^-}^{\text{LiC}_6}$$
 (27)

which can be compared to Eq.(4).

At that stage, the system is that given by Cell III.

Cell III:

 M^I | Li metal | Lithium electrolyte | Li_{UPD} | LiC_6 | M^{II} .

and is governed by following Nernst equation (similar to Eq. 6)

$$\phi^{S} - \phi^{LiC_{6}} = \left(\mu_{Li_{UPD}} - \mu_{Li^{+}}^{o,S} - \mu_{e^{-}}^{LiC_{6}}\right) / F - \frac{RT}{F} lna_{Li^{+}}^{S}$$
 (28)

By substituting in Eq. 8, we finally show that Cell III voltage is

$$[E]_{\text{vs Li}^+/\text{Li}} = \phi^{\text{M}^{\text{II}}} - \phi^{\text{M}^{\text{I}}} = (\mu_{\text{Li}}^- \mu_{\text{Li}_{\text{UPD}}})/F$$
 (29)

Large UPMD favours monolayer deposition and small UPMD favours 3D nucleation. As shown in Figure 1a, the potential is positive about 80 mV at the start of the UPMD and reaches zero once a lithium metal film or lithium 3D islands start to grow.

4. Discussion and scope

The understanding of graphite as a negative electrode material has been refined through multiple characterisation techniques and modelling, highlighting the nature of the Li-C interaction at the atomic scale, the staging phenomenon occurring upon lithium intercalation at the lattice scale, and the electrodeposition of lithium on graphite particles.

Describing the energy band structure of the LiC₆ lithium-graphite intercalation compound, Holzwarth and Rabii²² highlighted a remarkable charge transfer between the lithium 2s and graphite π^* orbitals. Although electrons from the Fermi level exhibited a negligible Li 2s character, the covalent nature of the bond was observed in other electronic states. Later, Hazrati *et al.* analysed the Li_{0.5}C₆ and LiC₆ intercalation compounds using Van der Waals density functional theory (DFT) compared to pristine graphite²³. Based on phonon densities of states, vibrational modes clearly involve mixed contributions from lithium and carbon, supporting a partial charge transfer between the two entities.

Ultimately, as described by Kganyago and Ngoepe $^{24}_{\text{low}}$ in lithiume graphite intercalation compounds such as 150 Me phase of the phase of t

At the lattice scale, Weng et al.26 examined the staging structure of graphite both macroscopically (XRD) and microscopically (cryo-TEM), proposing a revised model of lithiation. Their study showed that all stages of lithiated graphite exhibit a long-range order that can be characterised by X-ray or neutron diffraction. This macroscopic order tends to form phase domains, consistent with Daumas-Hérold model. However, each stage of lithiated graphite consists of a mixture of microscopic domains—specifically, stage II is composed of a mixture of stage III and stage I forming domains. This proposed "localiseddomains" model is supported by DFT calculations, which highlight the metastable nature of the various lithiation stages. Consequently, disproportionation of stages is more favourable, reinforcing the microscopic observation of domain mixtures. Gao et al. discussed the interplay between lithium intercalation and plating based on operando microscopy measurements²⁰. Thermodynamically, lithium plating is initiated when the graphite voltage drops around 0 V (vs Li⁺/Li). Under kinetic limitations, since lithium solid diffusion within individual graphite particles constrains the system, the authors demonstrated that the sufficient condition to trigger lithium plating is the lithium concentration at the particle surface. If the lithium concentration reaches saturation ($c\square = c\square$, max), lithium plating becomes more favourable than intercalation. In realistic systems (i.e. porous electrodes), the kinetic limitation arises from electrolyte diffusion, making the lithium concentration in the electrolyte solution the critical factor. When lithium depletion is too severe ($c\Box \rightarrow 0$), lithium plating is favoured. Most of the literature is focused on the structural aspects of the graphite lithiation processes. Here, we have focused on the potential-charge relationship. Figure 1a can be described as a potentiometric titration curve of the different phases. When, the graphite presents some solid solution properties, the Nernst equation for ion transfer reactions (eq.(10)) provides the potential response. When a solid phase starts to precipitate, e.g. LiC₃₆ or LiC₁₂, this equation is still valid but the concentration of "mobile" lithium ions in the remaining solid solution should be used. When solid phases are present, for x >

Stricto sensu, neither the adsorption nor the ion transfer reactions are redox reactions, meaning that graphite itself is not an anode. Only the electrodeposition involving the reduction of solvated lithium cations by UPMD or plating is a redox reaction; in this case, the electrode functions as a true anode, but it is

0.5) the potential is constant as given by eq.(26).

ARTICIF

composed of the pure "metallic" LiC_6 phase rather than graphite. Otherwise, the graphite electrode operates as a "volumic capacitor".

According to IUPAC¹⁹, an anode is defined as 'the electrode where oxidation occurs,' whereas a cathode is 'the electrode where reduction takes place.' Furthermore, oxidation is formally described as 'the complete removal of one or more electrons from a molecular entity or an increase in the oxidation number of any atom within a substrate,' while reduction represents the reverse process.

Thus, from a strict electrochemical perspective, it can be questioned if the negative graphite electrode is truly an anode?

Furthermore, according to the authoritative IUPAC nomenclature, batteries are defined as "devices that store energy to later be converted into electricity using chemical reactions. During discharge of a battery, the anode undergoes an oxidation reaction, which produces electrons, and the cathode undergoes a reduction reaction, which absorbs electrons²⁷". According to this definition, if the graphite electrode does not qualify as an anode, the lithium-ion battery is not a battery.

Also, in a previous communication¹, we argued that the commonly referred "cathode material" is not a cathode, but rather a redox-active particle in solution, with the actual cathode being the carbon black particles.

There is therefore some major discrepancies between the IUPAC definitions consistently used in patent laws, and the terminology used in the many publications and patents on lithium-ion batteries. Perhaps, IUPAC should revise their definitions to avoid further confusion.

Conclusions

Open Access Article. Published on 30 Onkololeessa 2025. Downloaded on 09/11/2025 7:31:13 AM.

This article is licensed under a Creative Commons Attribution 3.0 Unported Licence

In conclusion, a thermodynamic approach has been used to define the Nernst equations describing the lithiation of a graphite electrode. The potential charge curve has been treated as a potentiometric titration of the different carbon sites. The different sequential mechanisms involved in this lithiation process can be summarised as follows:

- Adsorption of solvated lithium onto "negatively" charged graphite corresponding to the start of the blue zone in Figure 1a.
- Intercalation or "dissolution" of desolvated bare lithium cations in a "solid solution" exhibiting Nernstian behaviour. The potential varies logarithmically with the concentration of lithium cations "solvated" by graphite and is given by Eq. (20). Blue zone and grey zone in Figure 1a.
- 3. Formation of a solid LiC_{36} and LiC_{12} phase through a biphasic "solid solution-solid" reaction. The potential remains independent of the lithium concentration in the electrolyte solution, but a logarithmic variation with the Li^+ concentration in the solid solution exists

and is given by Eq. S6 (Supporting Information). Green zones in Figure 1a. DOI: 10.1039/D5EB00202H

Journal Name

- 4. Formation of a solid LiC₆ phase through a biphasic solid-solid reaction. The potential is also independent of the lithium concentration in the electrolyte solution. Yellow zone in Figure 1a.
- Under potential deposition of Li atoms on LiC₆. The last white zone in Figure 1a, which can be followed by further electroplating.

Another aspect of this work is about the use of the authoritative IUPAC definitions, which are accepted by regulatory bodies. Indeed, following the electrochemical analysis presented above, it can be questioned if the negative graphite electrode is truly an anode?

Author contributions

The authors all contributed to the elaboration of this electrochemical model of the graphite electrode through many discussions. CR & HHG were responsible for the redaction of the article.

Conflicts of interest

There are no conflicts to declare.

Data availability

Not applicable.

Acknowledgements

The PhD thesis of C. Renais is financed by the Region Auvergne Rhône-Alpes (Pack Ambition Recherche 2021 – Projet IsoBATT). F.ElBachraoui wishes to thank MSN-UM6P and the Office Chérifien des Phosphates (OCP) for financial support.

References

- P. Peljo,, C. Villevieille and H.H.Girault. Energy Environ. Sci., 2025. 18, 1658.
- H. Zhang, Y. Yang, D. Ren, L. Wang and x- He, Energy Storage Mater, 2021, 36, 147.
- N Daumas and A. Hérold, CR Acad Sci Paris Ser C, 1969, 268, 373.
- U. Hofmann and W. Rüdorff, Trans Faraday Soc., 1938, 34, 1017.
- C. Renais, M.Mirolo, M. Servajon, J. Drnec, F. Alloin and C. Villevieille. Chem. Mater., 2025, 37, 5647.
- W.R. McKinnon, Insertion electrodes I: Atomic and electronic structure of the hosts and their insertion compounds. in *Solid State Electrochemistry* (ed. Bruce, P. G.) 163–198 (Cambridge University Press, 1994). doi:10.1017/CBO9780511524790.008.
- A. Van Der Ven, J. Bhattacharya and A.A.Belak, Acc. Chem. Res., 2013, 46, 1216.

ES Batteries Accepted Manuscript

View Article Online DOI: 10.1039/D5EB00202H

Journal Name ARTICLE

- 8. H.H. Girault, Electrochimie physique et analytique, EPFL Press,
- 9. S-Trasatti, J. Chem. Soc. Faraday Trans. 1, 1972, 68, 229
- M.D.Bhatt, M. Cho, M and K. Cho, J. Solid State Electrochem., 2012, 16, 435-441.
- 11. J.R. Dahn, Phys. Rev. B, 1991, 44, 9170.
- 12. H.J Lee, C.M. Pereira, A.F. Silvaand H.H. Girault, Anal. Chem., 2000, 72, 5562.
- 13. C. Sole, C., N.E. Drewett and L.J. Hardwick, Faraday Discuss, 2014, 172, 223.
- C. Didier, W.K. Pang, Z. Guo, S. Schmid, and V.K. Peterson, Chem. Mater., 2020, 32, 2518.
- C. Schmitt, A.Kube, N. Wagnerand K.A. Friedrich, ChemElectroChem., 2022, 9, 43.
- H.Fujimoto, M. Murakami, T. Yamanaka, K.Shimoda, H.Kiuchi, Z. Ogumi and T. Abe, J. Electrochem. Soc., 2021, 168, 080508 (2021).
- 17. H.Fujimoto, T. Yamaki, K.Shimoda, S. Fujinami, T. Nakatani, G.Kano, M. Kawasaki, Z.Ogumi and T.Abe, J. Electrochem. Soc., 2022. 169. 070507.
- S. Takagi, K.Shimoda, J. Haruyama, H. Kiuchi, K.I. Okazaki, T. Fukunaga, Z. Ogumi, T. Abe, Carbon, 2023, 215, 118414.
- The IUPAC Compendium of Chemical Terminology: The Gold Book. (International Union of Pure and Applied Chemistry (IUPAC), Research Triangle Park, NC, 2025). doi:10.1351/goldbook.
- T.Gao, Y. Han, D. Fraggedakis, S. Das, T. Zhou, C.N. Yeh, S. Xu, W.C. Chueh, J. Li and M.Z. Bazant. Joule, 2021 5, 393.
- D.M. Kolb, M.Przasnyski, and H. Gerischer, J. Electroanal. Chem. Interfacial Electrochem., 1974, 54, 25.
- N.A.W. Holzwarth and S. Rabii, Mater. Sci. Eng., 1977, 31, 195.
- E. Hazrati, G.A.De Wijs and G. Brocks, Phys. Rev. B, 2014, 90, 155448.
- 24. K.R. Kganyago and P.E. Ngoepe, Phys. Rev. B, 2003, 68, 205111.
- T. Insinna, E.N. Bassey, K. Märker, A. Collauto, A.L. Barra and C.P. Grey., Chem. Mater. 35, 5497-5511 (2023).
- S.Weng, S. Wu, Z. Liu, G. Yang, X. Liu, X. Zhang, C. Zhang, Q. Liu, Y. Huang, Y. Li, M.N. Ateş, D. Su, L.Gu, H. Li, L. Chen, R. Xiao, Z. Wang and X. Wang. Carbon Energy, 2023,5, e224
- 27. https://iupac.org/materialschemistryedu/energy/batteries/

View Article Online

DOI: 10.1039/D5EB00202H

This article is licensed under a Creative Commons Attribution 3.0 Unported Licence.

No primary research results, software or code have been included and no new data were generated or analysed as part of this perspective.